Materials Science Forum
ISSN: 1662-9752, Vol. 1062, pp 258-262
doi:10.4028/p-6410dm

Submitted: 2021-10-07
Revised: 2022-02-09
Accepted: 2022-03-07
Online: 2022-05-31

Transmission Electron Microscopy Study of Single Shockley Stacking Faults in 4H-SiC Expanded from Basal Plane Dislocation Segments Accompanied by Threading Edge Dislocations on Both Ends

Johji Nishio[1,a*], Chiharu Ota[1,b] and Ryosuke Iijima[1,c]

[1]Corporate Research & Development Center, Toshiba Corporation, 1 Komukai Toshiba-cho, Saiwai-ku, Kawasaki 212-8582, Japan

[a]johji.nishio@toshiba.co.jp, [b]chiharu.ota@toshiba.co.jp, [c]ryosuke.iijima@toshiba.co.jp

Keywords: single Shockley stacking fault, transmission electron microscopy, UV illumination.

Abstract. Double-rhombic shaped single Shockley stacking faults (1SSFs) were considered to have a converted threading edge dislocation (TED) on the shallower side of the initial basal plane dislocation segments. However, the structural analysis using transmission electron microscopy (TEM) revealed other possible configuration of the double-rhombic 1SSFs expanded from basal plane dislocations (BPDs) of which both ends were connected with two TEDs.

Introduction

Forward voltage degradation, which is observed mainly in bipolar devices and also in MOSFETs fabricated on 4H-SiC with a p-n junction, is widely known to be attributable to the expansion of 1SSFs in the epitaxial layer that originate from BPDs. Although many studies have proposed concepts for preventing the expansion of BPDs, such as reducing the minority carrier lifetime in the recombination-enhancing layers [1], BPDs are still present in commercially available epitaxial layers and cause variation in the threshold current density for 1SSF expansion.

Structural analysis is considered the key to better understanding how easily 1SSFs expand. We therefore previously investigated differences in the structure of partial dislocations (PDs) surrounding 1SSFs that had considerably different threshold current density for expansion [2]. We also examined PD combinations to determine whether they can expand even after the PD lines have been bent by the step-flow of the epitaxial growth [3,4]. In addition to the commonly observable triangular 1SSFs, different type of triangular 1SSFs that have right-angle on the deeper side of the epilayer and generated from short BPD segments were studied and the BPD was found to have TEDs on both ends [5]. Previous studies explored that the half-loop arrays of the dislocations [6,7] consist of short BPD segments accompanied by two TEDs to the epilayer surface on both ends.

In this study, we investigated the structure of double-rhombic 1SSFs to identify Burgers vectors and core species of the composing partial dislocations (PDs) and found that these is another type of BPD segment that has TEDs on both ends but one of which connected to the TED from the deeper side of the epilayer.

Experimental

Two types of double-rhombic 1SSFs (which we label 1SSF-A and 1SSF-B) were selected by photoluminescence (PL) imaging and expanded by UV illumination for 30 min (1.53 W/cm^2). Structural analysis was carried out by plan-view and cross-sectional transmission electron microscopy (TEM). To examine the fine structure of BPDs and 1SSFs, TEM sample preparation must first be performed by a focused ion beam (FIB) technique. For this, the depth of the 1SSF in the epilayer need to be determined precisely. Estimation from PL imaging can be misleading in terms of depth, because the shallowest ends of the BPDs are not always located at the very surface of the epilayer. Therefore, in this work, preliminary 1st cross-sectional TEM specimens were sampled in locations that contained identical 1SSFs but away from the areas where structural analysis was desired. Based on the 1SSFs depth results, plan-view TEM samples were prepared by FIB. The $\boldsymbol{g \cdot b}$ analysis was performed and Burgers vectors, $\boldsymbol{b}$, were obtained by the extinction rule. From the plan-view TEM images, different

sampling points were determined for the following analyses of 2nd cross-sectional TEM and cross-sectional scanning TEM (STEM) for high-resolution high-angle annular dark-field STEM (HAADF-STEM). Bright-field (BF) cross-sectional TEM images give information about how the BPD segments are connected with threading dislocations at each end. The HAADF-STEM images help determine the core species of PDs. The experimental procedure employed in this work is summarized in Fig. 1.

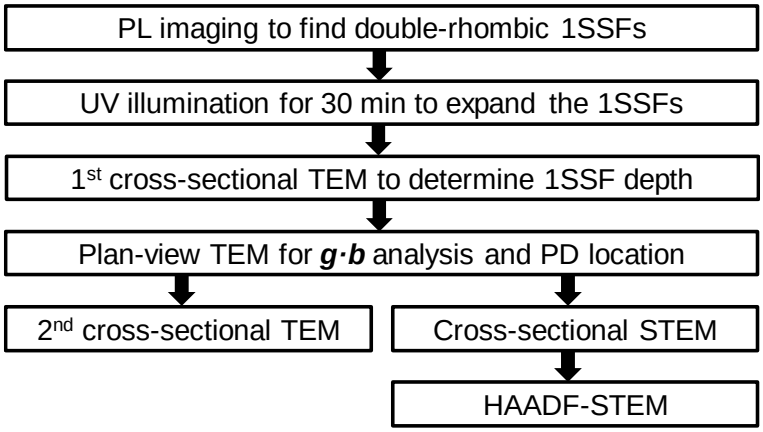

Fig. 1 Experimental procedure

Results and Discussion

Measurement of 1SSF depths by 1st cross-sectional TEM. Figures 2 and 3 show PL images and composite SEM images indicating the 1st cross-sectional TEM sampling positions (dashed light-blue rectangles) and areas of 1SSF-A and 1SSF-B observed by plan-view TEM (dashed yellow rectangles), respectively. BF-TEM images acquired with a slight inclination of the sample toward the [0001] direction from the [-1100] zone axis for maximized contrast of 1SSFs. Corresponding 1SSF depths were found to be 3.21 and 4.36 μm for 1SSF-A and 1SSF-B, respectively. Using these values, plan-view TEM samples were cut and thinned from the dashed yellow rectangle areas shown in Figs. 2(c) and 3(c).

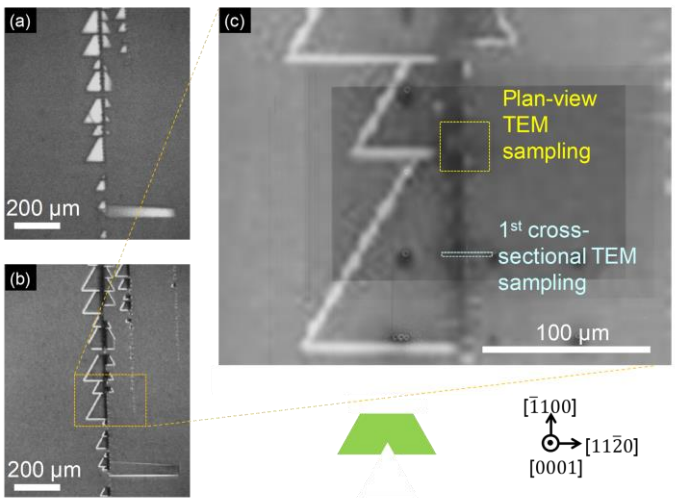

Fig. 2 PL and composite SEM images of 1SSF-A: (a) 420 nm BPF, (b) 750 nm HPF, and (c) composite of (b) and an SEM image.

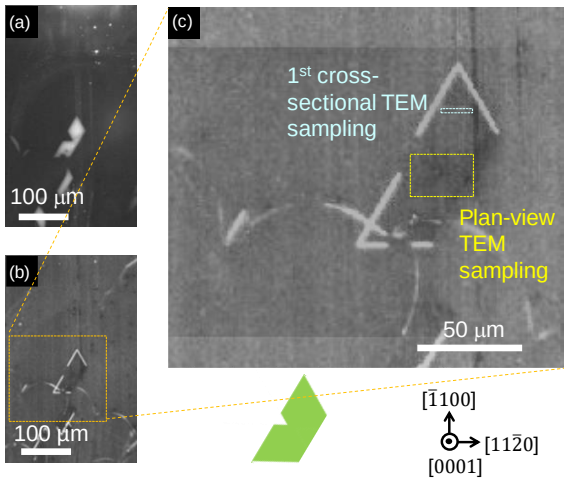

Fig. 3 PL and composite SEM images of 1SSF-B: (a) 420 nm BPF, (b) 750 nm HPF, and (c) composite of (b) and an SEM image.

Burgers vector determination by *g·b* contrast analysis. The Burgers vectors for PDs surrounding 1SSF-A and 1SSF-B were determined based on the plan-view TEM images by the extinction rule under two-beam conditions using different ***g*** vectors on the specimens sampled at the yellow-dashed lines in Fig. 2(c) and Fig. 3(c), respectively. Figure 4 shows the results of ***g·b*** contrast analysis for

1SSF-A. Although 1SSF-A must have contracted and changed its shape [4], the contrast of each dislocation line disappeared when ***g*** = -2110 and 1-210 on the left (Fig. 4(b)) and right (Fig. 4(c)) dislocation loops, respectively. Because TEDs are observed as beard-like lines [2] in general plan-view BF-TEM as in Figs. 4 and 5, we considered the regions marked by the dark arrows correspond to TEDs and they are considered to be the edge positions of the initial unexpanded BPD segment. The structural information on 1SSF-A was summarized in Fig. 4(d). Here, in simplicity, the green dashed line in Fig. 4(d) represents the estimated initial BPD as a simple straight line. Figure 5 shows the results of ***g·b*** contrast analysis for 1SSF-B. Also, 1SSF-B must have contracted and changed the shape, it seemed to have also two TEDs. The TED on the [11-20] side, the upper and lower line

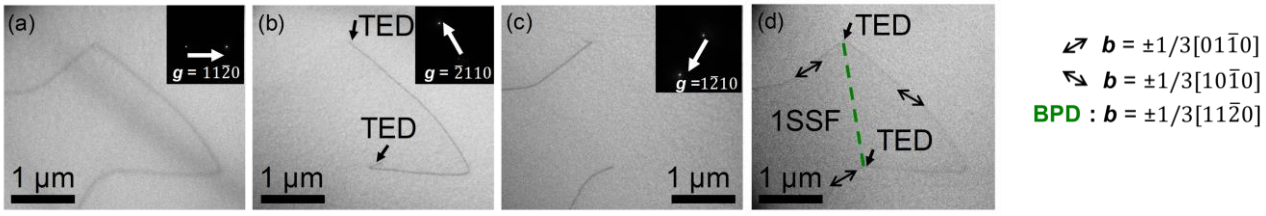

Fig.4 Plan-view BF-TEM results for 1SSF-A (part where TEDs were included): (a) ***g*** = 11-20, (b) ***g*** = -2110, (c) ***g*** = 1-210, and (d) ***b*** of PDs and unexpanded BPD.

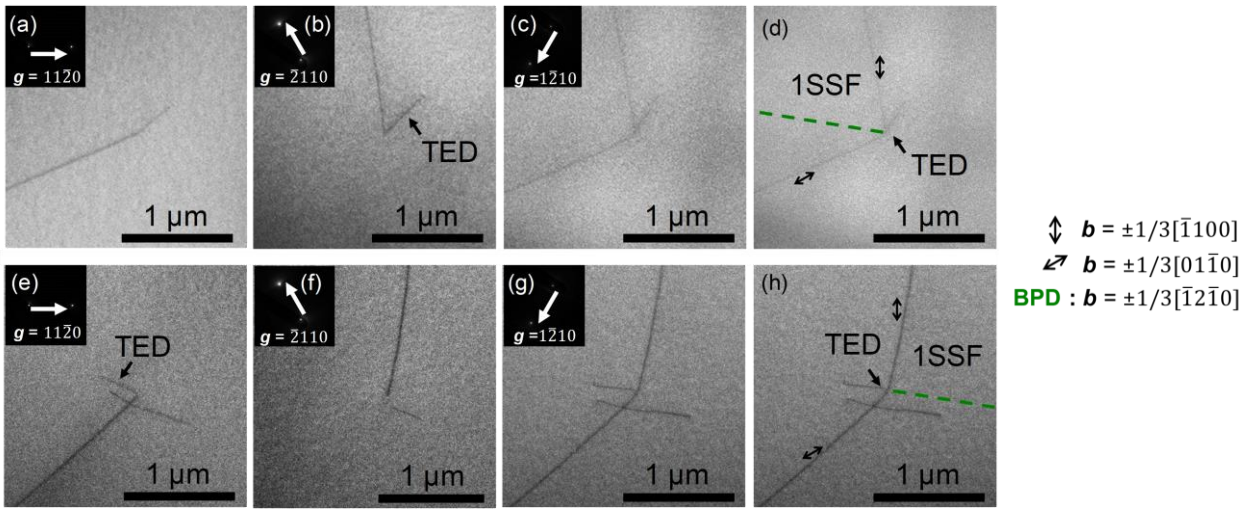

Fig.5 Plan-view BF-TEM results for 1SSF-B (parts where TEDs were included): (a)-(d) around the [11-20] side of TED, (e)-(h) around the [-1-120] side of TED, (a) and (e) ***g*** = 11-20, (b) and (f) ***g*** = -2110, (c) and (g) ***g*** = 1-210, and (d) and (h) ***b*** of PDs and unexpanded BPD.

contrast disappeared when ***g*** = 11-20 and -2110, respectively as seen in Fig. 5(a) and (b). On the other hand, the TED on the [-1-120] side, the same tendency found in Fig.5(a) and 5(b) also appeared as shown in Fig. 5(e) and 5(f). Therefore, the structural information on 1SSF-B was summarized in Fig. 5(d) and (h). The initial BPD for 1SSF-B have been found to have its ***b*** of ± (1/3) [-12-10].

2nd cross-sectional TEM results. Figures 6 and 7 show cross-sectional TEM images of 1SSF-A and 1SSF-B in FIB samples that were cut to include the TEDs at both ends of the unexpanded BPD segments. In Fig. 6, both ends of the 1SSF-A were found to be connected to TEDs where the unexpanded BPD segment had been previously. This result agrees well with previous etch-pit and PL studies on the half-loop arrays [6,7]. In the case of 1SSF-B, the distance between the two TEDs was so far that we could not acquire an image of them in a single shot. Both ends of 1SSF-B are shown in Fig. 7, where we can see that the deeper end of 1SSF-B is connected to a TED that might have come from the deep part of the epilayer, while the shallower end is connected to a TED that might have penetrated to the surface of the epilayer. We could explain that the TED-BPD-TED conversion was

the result of unstable step flow that once bent TED to BPD and converted back to TED. This speculation was derived from the fact that the region in Fig. 7 was close to the edge of the wafer and the angle between (0001) and TEDs are so different between Figs. 6 and 7, but further statistical study is necessary.

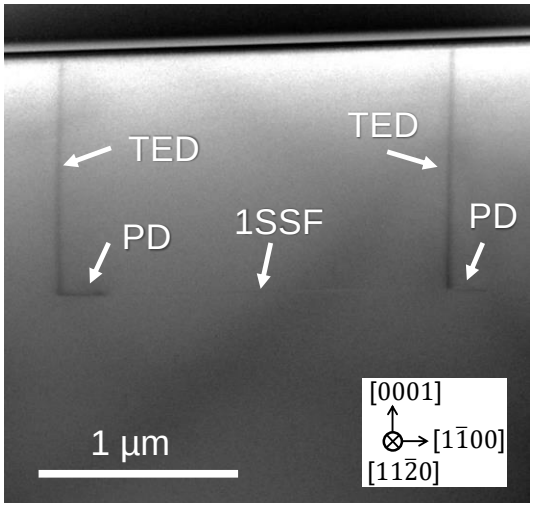

Fig.6 2nd cross-sectional BF-TEM image of 1SSF-A.

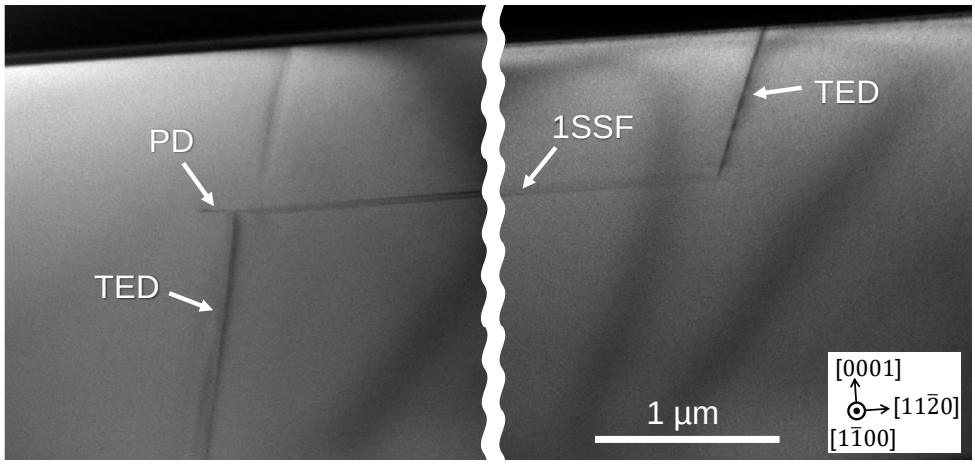

Fig.7 2nd cross-sectional BF-TEM image of 1SSF-B.

Cross-sectional STEM and HAADF-STEM. At the corresponding boundaries of the 1SSFs, different specimens for cross-sectional observation were cut perpendicular to the PD lines by FIB and HAADF-STEM analysis was performed with finish-to-start using the right-hand definition in the perfect crystal convention. The uniquely determined ***b*** and core species for each PD are shown in three-dimensional schematics shown in Figs. 8 and 9, which speculatively show the unexpanded BPDs (Fig. 8(a) and Fig. 9(a)) and present a summary of the analysis results (Fig. 8(b) and Fig. 9(b)).

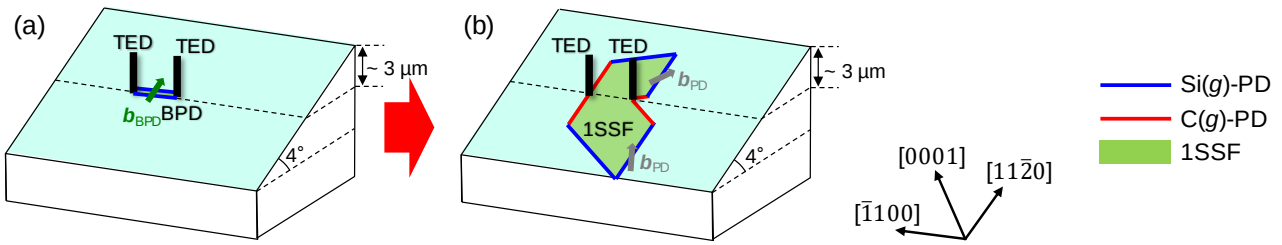

Fig.8 Schematics of 1SSF-A structure: (a) unexpanded BPD, and (b) analysis results explaining PL imaging.

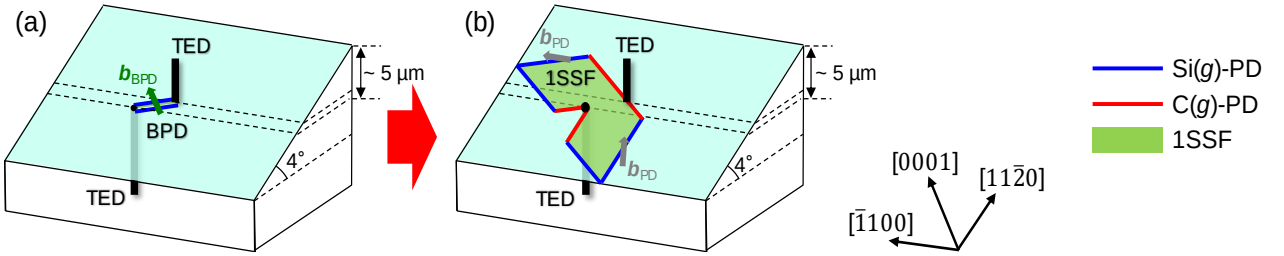

Fig.9 Schematics of 1SSF-B structure: (a) unexpanded BPD, and (b) analysis results explainingr PL imaging.

The inclination angle of DRSF was found to be determined by ***b***. Only the HLA-type BPD can form the DRSF as shown in Figs. 2 and 8 or upside-down. Although structural identification of the classified structures [8,9] suggests the possible assignment of the BPD segments, preventing the formation of these kinds of BPD segments remains a major issue to be solved.

Summary

We investigated the structure of double-rhombic 1SSFs to identify Burgers vectors and core species of the composing PDs. From the results, we found that these are other types of BPD segments from the previously found ones in triangular 1SSF expanded toward substrate side [5] that had TEDs on both ends; one is HLA-type and another is different TED-BPD-TED origin.

References

[1] T. Tawara, et al., J. Appl. Phys. 120 (2016) 115101.

[2] J. Nishio, A. Okada, C. Ota, and R. Iijima, J. Appl. Phys. 128 (2020) 085705.

[3] J. Nishio, A. Okada, C. Ota, and R. Iijima, Jpn. J. Appl. Phys. 60 (2021) SBBD01.

[4] J. Nishio, C. Ota, and R. Iijima, J. Appl. Phys. 130 (2021) 075107.

[5] C. Ota, J. Nishio, A. Okada, and R. Iijima, J. Electron. Mater. 50 (2021) 6504.

[6] S. Ha, H. J. Chung, N. T. Nuhfer, and M. Skowronski, J. Crystal Growth 262 (2004) 130.

[7] N. Zhang, et al., Appl. Phys. Lett. 94, 122108 (2009).

[8] A. Iijima, I. Kamata, H. Tsuchida, J. Suda, and T. Kimoto, Philos. Mag. 97, 2736 (2017).

[9] H. Matsuhata and T. Sekiguchi, Philos. Mag. 98, 878 (2018).